AI-Enhanced Generative Design for Efficient Heat Exchangers in Thermoelectric Generators: Revolutionizing Waste Heat Recovery in Thermoelectricity

Andrew Robert Martin Hughes, Baljit Singh Bhathal Singh[*], Muhammad Fairuz Remeli
School of Mechanical Engineering, College of Engineering, Universiti Teknologi MARA, 40450 Shah Alam, Selangor, MALAYSIA
[*]baljit@uitm.edu.my

Guilherme Fidelis Peixer
POLO – Research Laboratories for Emerging Technologies in Cooling and Thermophysics, Department of Mechanical Engineering, Federal University of Santa Catarina, Florianópolis, SC, BRAZIL

Wandeep Kaur Ratan Singh
Center of Artificial Intelligence, Faculty of Information Science and Technology, Universiti Kebangsaan Malaysia, 43600 Bangi, Selangor, MALAYSIA

ABSTRACT

Thermoelectric generators (TEGs) offer the potential for converting waste heat into electricity, but their efficiency, particularly at low temperatures, remains inadequate. Plate-Fin Heat Exchangers (PFHEs) in TEG systems are not fully optimized, resulting in limited efficiency and applicability. The low conversion efficiency of TEGs means only a small fraction of waste heat is utilized, posing challenges to their long-term viability. While Genetic Algorithms (GAs) have shown promise in optimizing heat exchanger designs, advanced methods like Non-dominated Sorting Genetic Algorithm II (NSGA-II) have yet to be fully applied for PFHE TEG design. This study addresses these challenges by using NSGA-II, combined with a semi-empirical model, to optimize PFHE design in TEG systems. The optimization focuses on refining fin design parameters such as number, width, and height while adhering to

ISSN 1823-5514, eISSN 2550-164X
Received for review: 2024-07-18
Accepted for publication: 2024-10-03
Published: 2024-11-15

https://doi.org/10.24191/jmeche.v13i1.2935

constraints on fin area and pressure drop. The optimized design achieved a 3.94% increase in output power and a 1.72% increase in efficiency at 373.15 K, with conversion efficiency rising by 154.74% and maximum output power by 549.64% at 428.15 K. In conclusion, this research bridges the gap by applying NSGA-II to enhance PFHE design in TEGs, significantly improving performance and sustainability. Future work will explore alternative models and further optimization to achieve even higher efficiencies.

Keywords: *Thermoelectric Generator; Artificial Intelligence; System Optimization; Plate-Fin Heat Exchanger; Waste Heat Recovery*

Introduction

Energy efficiency and Waste Heat Recovery (WHR) are vital in today's industrial processes due to the demand for sustainable energy. Waste heat, a byproduct of these processes, is a largely untapped resource that, if recovered, can reduce greenhouse gas emissions and improve energy efficiency, aligning with global sustainability goals. Plate-Fin Heat Exchangers (PFHEs) and Thermoelectric Generators (TEGs) are key technologies in WHR. PFHEs are valued for their compact design and high performance, while TEGs convert waste heat directly into electricity via the Seebeck effect. By leveraging Artificial Intelligence (AI), the efficiency of PFHEs and TEGs can be significantly enhanced, positioning TEGs as a viable solution for boosting energy recovery in industrial settings.

According to Khan et al. [1], PFHEs play an essential role in industrial waste heat recovery owing to their compact construction and excellent efficiency and are extensively used in process industries such as petrochemical, chemical, and many more. However, despite their effectiveness, challenges such as indirect power generation and costly installation and maintenance requirements are the key issues as stated by Miao et al. [2]. Thus, installing TEGs would be a feasible option, recovering more than 60% of energy loss as demonstrated by Nourdanesh and Kantzas [3]. Garud et al. [4] highlighted that TEGs are Seebeck effect-powered devices that directly transform waste heat into electricity without the need of moving components, lowering dependency on fossil fuels and associated Green House Gasses (GHG) emissions.

Genetic Algorithms (GAs), which were inspired by Charles Darwin's theory of evolution [5], are known as a powerful optimization approach that initially developed in the 1950s. As a result, the bio-inspired tool has grown to tackle problems in a variety of disciplines, including optimization and machine learning presented by Katoch et al. [6]. With that being said, GA excels in automated optimization searches, providing a global tool for heuristic search capabilities. GAs are a popular algorithm that is known for their simplicity and

versatility in solving a wide range of issues, as well as their efficacy in identifying robust solutions.

According to Song et al. [7] and Meng et al. [8], recent advancements in Multi-Objective Optimization (MOO) have significantly enhanced the evaluation and improvement of heat exchanger performance, utilizing various thermodynamic and economic indices. The Non-dominated Sorting Genetic Algorithm II (NSGA-II), an evolutionary algorithm based on GA, is particularly adept at managing complex, multi-objective optimization tasks. It is crucial for optimising PFHE in TEGs, where it balances conflicting objectives, such as maximizing efficiency and power output while minimizing pressure drops. Unlike its predecessor, the GA, NSGA-II introduces a fast and elitist sorting approach that categorizes solutions into different fronts based on dominance.

A multi-objective GA excels in addressing these challenges, offering distinct advantages over traditional mathematical programming as highlighted by Damavandi et al. [9]. The algorithm's ability to manage multiple conflicting objectives simultaneously is invaluable, as it allows for the identification of designs that achieve the best balance between competing factors, as argued by Hajabdollahi et al. [10]. This capability is vital in industrial, aerospace [11] and automotive [12] applications, where seamlessly integrating technical performance with economic and operational constraints is essential.

Furthermore, the integration of semi-empirical models with NSGA-II marks a significant advancement in enhancing TEG performance. According to Lan et al. [13], these models blend robust theoretical principles with empirical data, considerably improving the accuracy of thermal behaviour predictions for PFHEs. Adjustments to critical design parameters, informed by empirical observations such as temperature difference values and heat transfer rates, ensure that the optimization outcomes are both practically feasible and theoretically valid.

This study leverages AI, specifically NSGA-II, to enhance the efficiency of PFHEs in TEGs for low-temperature WHR, with a particular focus on using wastewater as the heat source. The aim is to reduce energy consumption, lower GHG emissions, and promote sustainable energy practices. Additionally, it seeks to cut industrial operational costs and align with broader sustainability goals, contributing to several UN Sustainable Development Goals (SDGs), including SDG 7 (Affordable and Clean Energy), SDG 9 (Industry, Innovation, and Infrastructure), SDG 11 (Sustainable Cities and Communities), SDG 12 (Responsible Consumption and Production), SDG 13 (Climate Action), and SDG 15 (Life on Land).

The research also underscores the substantial untapped potential in recovering energy from these processes, which have considerable environmental impacts. Traditional combustion processes, which consume over 80% of energy, generate significant amounts of waste heat, making its recovery essential for sustainable energy production and reducing GHG

emissions, as noted by Zhu et al. [14]. Fossil fuel-based power generation typically produces about 60% of its energy as waste heat, yet only around 7% is currently recovered, as highlighted by Chen et al. [15], and Miao et al. [2]. By recovering low-temperature waste heat, especially from hot wastewater, this study not only conserves water but also promotes sustainable management practices that further reduce GHG emissions.

In conclusion, this project combines technological innovation with social effects, economic feasibility, and environmental awareness to tackle the critical challenges of enhancing energy efficiency and low-temperature WHR in industrial operations.

Methodology

Semi-empirical model

This research builds on a semi-empirical model that replicates a physical system from a prior study by Chen et al. [15] to evaluate a low-temperature waste heat recovery (WHR) system as depicted in Figure 1.

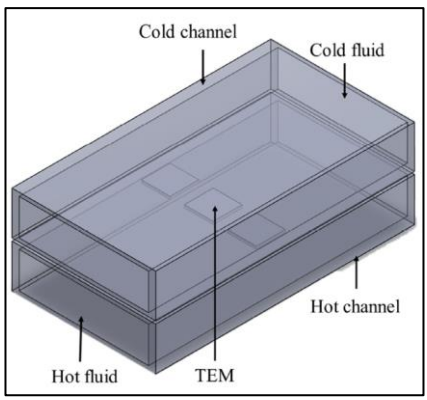

Figure 1: TEG PFHE model structure [15]

The system comprises a waste heat channel and a cooling channel, each measuring 36 cm × 20 cm × 6 cm, and includes several plate fins and thermoelectric generators (TEGs). Positioned between the waste and cooling channels, the TEGs use the temperature gradient across thermoelectric materials to convert thermal energy to electrical energy via the Seebeck effect. The focus of this study is to optimize the system by modifying the number and dimensions of the fins and comparing these changes to a previous study that used a Reynolds number of 1000. This study also explores the effects of altering the configurations and number of TEGs and the dimensions of the

channels such as the width and length on the system's efficiency and maximum power output.

The primary sources of low-temperature waste heat are air or water, which are common cooling mediums in most heat exchange systems as stated by Zou et al. [16]. Consequently, water is used exclusively as the working fluid in these simulations. Previous findings from He et al. [17] indicated that TEGs in a counter-flow configuration produced 15% more power than those in a co-flow setup, concluding the use of counter-flow in this study. The water properties such as density, viscosity, thermal conductivity, and specific heat are presented in Table 1.

The study employs TEGs also known as Thermoelectric Modules (TEMs) that are commercial-sized rectangular modules (4 cm × 4 cm × 0.375 cm), similar to TEC1-12706 conducted by Chen et al. [18], consisting of 127 pairs of p-type and n-type elements made of Bi_2Te_3, with detailed properties listed in Table 1. The power output from the TEGs is derived from the temperature difference between the hot and cold sides of the TEM. To align with practical scenarios in low-temperature waste heat recovery, three TEGs are used, replicating the configurations from previous studies for equal comparison.

Table 1: Properties of the TEG material and water [15]

Parameters	Unit	Value
Parameters of TEM		
Seebeck coefficient	$V \cdot K^{-1}$	$S_p = -S_n = 226.8 \times 10^{-6}$
Thermal conductivity	$W \cdot m^{-1} \cdot K^{-1}$	$k_p = k_n = 1.52$
Resistivity	$\Omega \cdot m$	$\rho_p = \rho_n = 1.447 \times 10^{-5}$
Parameters of water		
Density	$kg \cdot m^{-3}$	998.2
Specific heat at constant pressure	$J \cdot kg^{-1} \cdot K^{-1}$	4182
Thermal conductivity	$W \cdot m^{-1} \cdot K^{-1}$	0.6
Viscosity	$kg \cdot m^{-1} \cdot s^{-1}$	0.001003

To boost the efficiency of the TEGs, aluminium plate-fins are integrated into the waste heat channel. Based on prior studies, each fin is sized at 3 cm × 0.2 cm × 4 cm (length × width × height). Moreover, the impact of fin geometry on thermoelectric performance revealed that increasing fin length had a negligible effect on performance enhancement at low flow rates as proven by Jang et al. [19], therefore, the fin length is fixed at 3 cm for the optimization process. Thus, this study only further optimizes the width, height, and number of fins, whereas the previous study has found that the optimal fin count for achieving the highest conversion efficiency and maximum output power is 27. Moreover, this study examines the impact of varying the number of TEGs and the dimensions of the channels specifically the width and length

alongside modifications to the number and dimensions of fins, on the system's conversion efficiency and maximum power output.

The physical phenomenon is assumed to be in a steady state. The Reynolds number (*Re*) of a flow in the channel is defined as:

$$Re = \frac{\rho V D}{\mu} \tag{1}$$

where ρ, V, D, and μ represent the fluid density, velocity, hydraulic diameter, and dynamic viscosity, respectively. In this study, *Re* of 1000 are considered, indicating that the flows are laminar and incompressible. Thermal radiation and stress between materials are neglected. The hydraulic diameter is calculated using:

$$D_H = 4\left(\frac{Effective\ flow\ area}{Effective\ wetted\ perimeter}\right) \tag{2}$$

Since the hot channel includes plate-fins, the effective flow area is calculated by subtracting the plate-fin area from the hot channel area, and the effective wetted perimeter is found by adding the perimeters of the hot channel and plate-fins. In contrast, the cold channel, without plate-fins, has its hydraulic diameter calculated directly by:

$$D_C = \frac{2(Wc \times Hc)}{Wc + Hc} \tag{3}$$

where *Wc* and *Hc* are the width and height of the cold channel. In order to calculate the Nusselt Number (*Nu*), two criteria were satisfied such as Reynold Numbers, *Re* < 2300 and Prandtl Number, *Pr* > 0.7. Thus, the hydraulic diameter, *D* of Equation (2) and Equation (3), and the length of channels, *L* are used for this purpose. Therefore, the *Nu* correlation for laminar flow used for each channel, as defined by Gnielinski [20] is given as:

$$Nu_{lam} = \left\{Nu_{m,q,1}^3 + 0.6^3 + (Nu_{m,q,2} - 0.6)^3 + Nu_{m,q,3}^3\right\}^{\frac{1}{3}} \tag{4}$$

$$Nu_{m,q,1}^3 = 4.354 \tag{5}$$

$$Nu_{m,q,2} = 1.953\sqrt[3]{Re\ Pr\ (\frac{D}{L})} \tag{6}$$

$$Nu_{m,q,3} = 0.924\sqrt[3]{Pr}\sqrt{Re\,(\frac{D}{L})} \tag{7}$$

Upon determining the *Nu* from Equation (4), along with the hydraulic diameters of the channels and the thermal conductivity of water, the heat transfer coefficient is established as:

$$h = \frac{Nu\ K}{D} \tag{8}$$

The mass flow rate is given by:

$$\dot{m} = \rho\ V\ A \tag{9}$$

where *A* is defined as the effective flow area derived from both the hot and cold channels. Meanwhile, by using the mass flow rate from Equation (9) and the specific heat at constant pressure, *Cp*, the heat capacity rates are defined as:

$$C = \dot{m}\ Cp \tag{10}$$

The convective thermal resistance of the channels is then defined as:

$$R_{conv} = \frac{1}{h\ \times\ A} \tag{11}$$

Meanwhile, the thermal conduction resistance of the TEG is given by:

$$R_{TEG} = \frac{Thickness\ (w)}{K\ \times A} \tag{12}$$

The overall heat transfer coefficient, *U* is given by:

$$U = \frac{1}{Total\ Overall\ Thermal\ Resistance} \tag{13}$$

where the total overall thermal resistance is obtained by summing up the values obtained from Equation (11) and Equation (12). Thus, the Number of Transfer Unit, NTU is given as:

$$NTU = \frac{U\ \times\ A_{total}}{C_{min}} \tag{14}$$

The total area includes the total area of TEG used and the surface area of hot and cold channels, meanwhile, the C_{min} is obtained from Equation (10). The effectiveness, *e* for counterflow is expressed as:

$$e = \frac{(1 - \ exp(-NTU\ (1 - C))}{1 - C\ exp\ (-NTU\ (1 - C))} \tag{15}$$

The maximum heat transfer rate, Q_{max}, and actual heat transfer rate, Q_{actual} are given below:

$$Q_{max} = C_{min}\ (T_{h_{in}} - T_{C_{in}}) \tag{16}$$

$$Q_{actual} = e\ .\ Q_{max} \tag{17}$$

where $T_{h_{in}}$ and $T_{C_{in}}$ represent the inlet temperatures of the hot and cold channels, respectively. The temperature difference across the TEG is obtained by:

$$\Delta T_{TEG} = (T_{h_{out}} - T_{C_{out}}) \tag{18}$$

Meanwhile, the internal resistance of the TEG can be found using:

$$R_{int} = = \frac{p\ H}{A_{TEG}} \tag{19}$$

where ρ represents the electrical resistivity of the TEG, *H* represents the height or thickness of the TEG and A_{TEG} is the cross-sectional area of the TEG. This study assumes that thermoelectric materials have constant properties and ignores the Thomson effect. The output power, *P*, and maximum output power P_{max} produced by the TEG are obtained by:

$$\mathrm{P} = \left(\frac{S\ \Delta T_{TEG}}{(R_{int} + R_{ext})}\right)^2 \mathrm{x}\ R_{ext} \tag{20}$$

$$\mathrm{P_{max}} = \frac{S^2 {\Delta T_{TEG}}^2}{(4\ R_{int})} \tag{21}$$

where *S*, R_{int}, and R_{ext} are the Seebeck coefficient of the TEG (*S* = *Sp* - *Sn*), the TEG internal resistance, and the external load resistance, respectively. This study considered impedance matching to track the maximum output power, defined by:

$$R_{int} = R_{ext} \tag{22}$$

Impedance matching means that the internal resistance is equal to the external resistance. The maximum output power is obtained from Equation (21) under the impedance matching. In order to find the total maximum output power, it is required to multiply with the total number of TEGs used such as:

$$Total\ P_{max} = No.of\ TEG\ \times\ P_{max} \tag{23}$$

The maximum conversion efficiency of the TEG can be calculated by:

$$n = \frac{P_{max}}{Q_{actual}} \times 100 \tag{24}$$

The pressure drop of the hot side is calculated using:

$$\Delta P = f \times \frac{L}{D} \times \frac{\rho V^2}{2} \tag{25}$$

The variables *f*, *L*, *D*, *ρ*, and *V* represent the friction factor, length of the hot channel, hydraulic diameter of the hot side, density of water, and velocity on the hot side, respectively. Moreover, the Absolute Percentage Error (*APE*), followed by the Mean Absolute Percentage Error (*MAPE*) formula, used to quantify the accuracy of the semi-empirical model, are given as follows:

$$APE = \left|\frac{Experimental\ Value - Simulation\ Value}{Experimental\ Value}\right| \times 100 \tag{26}$$

$$MAPE = \frac{1}{n}\sum_{i=1}^{n} Absolute\ Percentage\ Error \tag{27}$$

where *n* is the number of data points. Finally, a weighted global criterion method was applied to determine the optimal design. The utility function was adjusted to accommodate the maximization of both objectives, as defined by:

$$O_c = \left\{\sum_{i=1}^{k} w_i\ [F^o - F_i(X)]^p\right\}^{\frac{1}{p}} \tag{28}$$

where O_c is the global criterion, w_i a vector of weights for each objective function, p is a coefficient to emphasize the minimization of one of the

objectives, F represents the Pareto optimal systems and F^o is the utopia point, which defined as:

$$F^o = [\max(p\_max), \max(efficiency\_\max)] \quad (29)$$

Non-dominated sorting genetic algorithm II

In this study, the NSGA-II algorithm is utilized for the multi-objective optimization of the TEG PFHE system. The Pareto front was generated using the NSGA-II evolutionary algorithm, which relies on biologically inspired operators such as mutation, crossover, and selection to determine the optimal solution. The entire optimization was conducted using Python 3.12.0 with the Pymoo package [21]. The flowchart outlines several processes aimed at maximizing both the thermoelectric power output and conversion efficiency of the TEG, as shown in Figure 2.

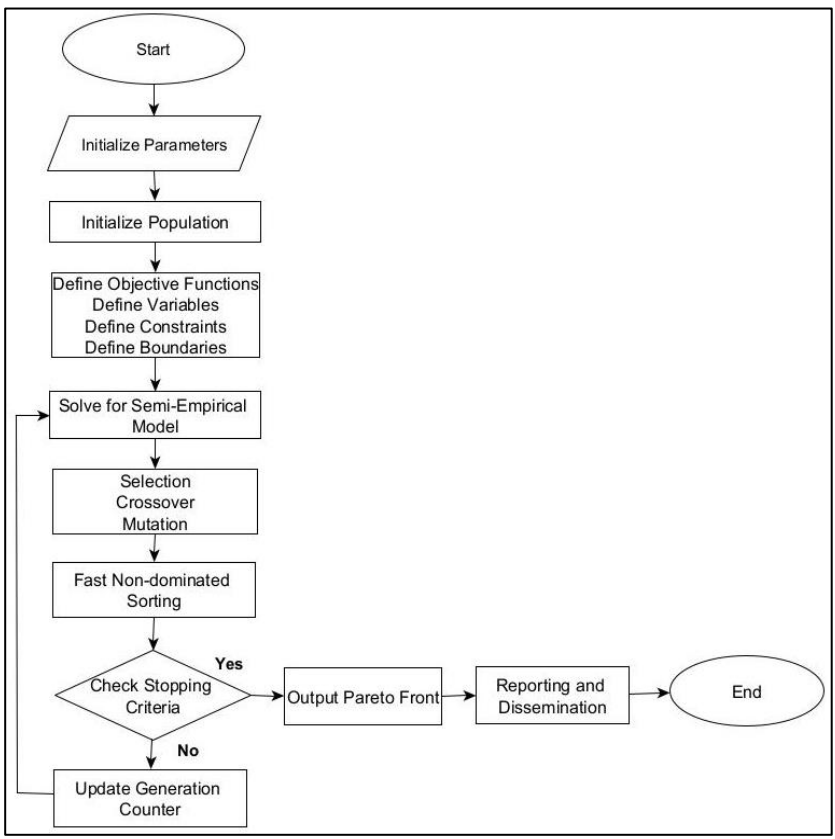

Figure 2: Flowchart for NSGA-II algorithm

Initially, the problem is defined with input parameters, two objective functions, and three variables representing the maximum output power and maximum efficiency of the TEG. The three design parameters include the number of fins (ranging from 25 to 65), fin width (0.1 cm to 0.5 cm), and fin height (2 cm to 5.5 cm), as depicted in Table 3. NSGA-II employs float random sampling to generate 300 new populations or solutions for each of the design parameters based on their maximum and minimum values during the optimization process. A semi-empirical model is then implemented to solve Equations (1) to (25) within the TEG PFHE system. For each iteration, a random population is created, and fitness scores are assessed. Individuals with the highest fitness scores are given preference for breeding.

Breeding is performed using Simulated Binary Crossover (SBX), where two offspring are produced from two parents. Two individuals are selected using the binary tournament mating selection, where each individual is compared first by rank and then by crowding distance as highlighted by Deb et al. [22]. After selection, the crossover sites are exchanged, creating new individuals or offspring. Genes are randomly mutated to introduce diversity into the population, using a method called polynomial mutation. Table 2 represents the settings used to operate the algorithm.

Fitness scores are then reassessed, and the fittest individuals proceed to the next generation through fast non-dominated sorting, for a total of 300 generations or iterations. The algorithm determines whether to continue based on the maximum number of generations (300) or convergence tolerance thresholds as can be seen in Table 2. If the stopping criteria are met, the process proceeds to output the Pareto front. This forms an evolution loop that includes selection, crossover, mutation, fitness evaluation, and reselection again.

For each generation, duplicates are eliminated to promote diversity. The simulated binary crossover specifies a crossover probability and a distribution index that determines how close the offspring solutions are to the parent solutions. The fitness of the new population is then evaluated, and the binary tournament mating selection is used again to select the fittest individuals for the next generation, ensuring the survival of the fittest.

The PFHE designs are refined by repeating the steps of checking stopping criteria, performing genetic operations, and updating the generation counter until the stopping criteria are met. Once the optimization process is complete, the optimized designs are compared with existing solutions. The Pareto front displays a set of optimal solutions that illustrate the trade-offs between multiple objectives. The use of two objective functions in NSGA-II results in a Pareto front where each performance factor is optimized to its maximum value.

Table 2: Settings of the algorithm

Parameter	Value	
Population size	300	
Number of offsprings	300	
Selection function	Binary tournament mating	
Crossover fraction	0.8	
Crossover function	Simulated binary crossover	
Mutation fraction	0.1	
Mutation function	Polynomial mutation	
Stopping criteria	Maximum generation	300
	Tolerance for design variables	1×10^{-8}
	Constraint violation tolerance	1×10^{-6}
	Tolerance for objective functions	1×10^{-6}

Table 3: Parameters used for the algorithm

Parameter	Unit	Value
Input		
Reynolds Number, *Re*		1000
Hot inlet temperature, T_{hin}	K	353.15
Cold inlet temperature, T_{cin}	K	303.15
Cold channel	cm	36 x 20 x 6
Hot channel	cm	36 x 20 x 6
Length aluminium plate fins	cm	3
Thermoelectric generator	cm	4 x 4 x 0.375
Variable range boundaries		
Plate-fin number		$25.0 \leq x \leq 65.0$
Fin width	cm	$0.1 \leq x \leq 0.5$
Fin height	cm	$2.0 \leq x \leq 5.5$
Constraints		
Plate-fin area space	cm^2	$x \leq 60$
Pressure drop	Pa	$x \leq 1$

Results and Discussion

Model validation

In numerical investigations, it is essential to ensure that the model and its settings are appropriately aligned with the problem to achieve reliable and accurate results. To validate the accuracy of the semi-empirical model before integrating it into the NSGA-II algorithm, the results were compared with the experimental data [15]. The semi-empirical model comprises Equations (1) to

(24), which are utilized to solve the total maximum output power and maximum conversion efficiency of the TEG PFHE system.

Based on Figure 3, the MAPE for the total maximum output power and maximum conversion efficiency based on Equations (26) to (27), is 5.37% and 1.29%, respectively. These values are both below 6%, effectively achieving numerical validation which is supported by Chen et al. [15], and Wang et al. [23]. This demonstrates that the modelling approach aligns with the problem, delivering accurate and reliable results. Consequently, this validated model will be used for the AI algorithm.

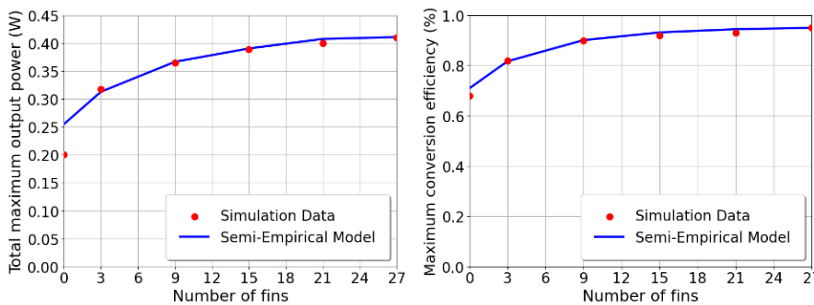

(a) (b)

Figure 3: Comparisons of semi-empirical model and experimental data (a) total maximum output power and (b) maximum conversion efficiency

Optimization results

The primary aim is to enhance the maximum output power and conversion efficiency of the TEGs of the PFHE. Based on the previous research [15], the results achieved a total maximum output power of 0.411 W, a maximum output power of 0.137 W, and a maximum conversion efficiency of 0.95% at 373.15 K using 27 fins, with a fin width and height of 0.002 m and 0.04 m, respectively. The Pareto front based in Figure 4 represents the set of optimal solutions generated by the NSGA-II.

The two objectives, maximizing output power and conversion efficiency, show a clear trade-off, where increasing one often reduces the other as shown in Figure 4. This trade-off is crucial for decision-makers, as it visually represents possible solutions, helping them choose the best configuration based on their needs. The spread and shape of the Pareto front demonstrate the NSGA-II algorithm's effectiveness in capturing a wide range of optimal solutions. With the right balance of design parameters, significant improvements in both power output and efficiency are achievable compared to baseline configurations.

A Weighted Global Criterion Method, which was used by Peixer et al. [24] and Marler et al. [25] was utilized to select the final design, using

Equations (28) to (29). The objective functions were normalized to dimensionless form, ensuring comparability across different units. The weights assigned to p_max (maximum output power) and efficiency_max (maximum conversion efficiency) were set to 0.5 each, indicating an equal emphasis on both objectives, and p was set equal to unity.

Thus, after optimization, the maximum conversion efficiency increased to 0.9663%, and the maximum output power rose to 0.1424 W. The optimal design identified included 64 fins, each with a width of 0.001 meters and a height of 0.0304 meters. This configuration was the most effective within the given constraints, achieving a fin area of 0.00195 m² and a pressure drop on the hot side of 0.94 Pa, all within the limits specified in Table 3, ensuring feasibility within the model.

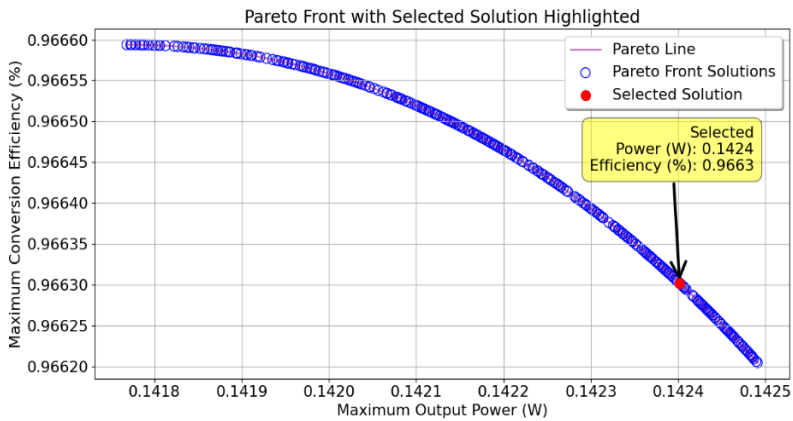

Figure 4: Resulting Pareto front of the MOO problem

Figure 5(a) shows how the algorithm converges to meet problem constraints over successive generations, ensuring solutions are both optimal and feasible. Figure 5(b) displays the hypervolume indicator, which measures the objective space covered by the Pareto front. An increasing hypervolume indicates effective exploration and improvement of solutions, demonstrating the robustness of the NSGA-II algorithm. After performing the main optimization, different scenarios were explored.

Figure 6 illustrates the effect of varying hot inlet temperatures on the balance between maximum output power and conversion efficiency during the MOO. Higher inlet temperatures shift the Pareto front towards increased power and efficiency, highlighting that elevated temperatures can significantly improve TEG system performance. This underscores the importance of temperature management in optimizing TEG systems and provides insights into the PFHE's thermal behaviour under different conditions.

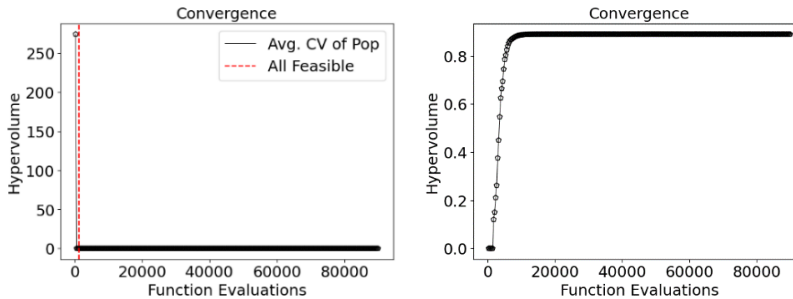

(a) (b)

Figure 5: Convergence analysis for (a) constraint satisfaction and (b) hypervolume of the algorithm

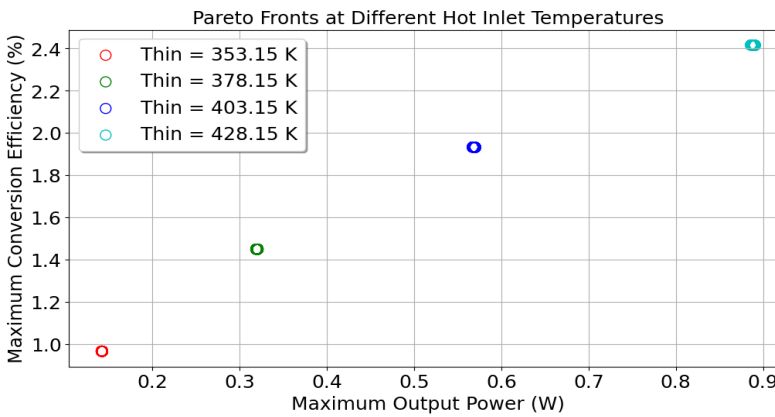

Figure 6: Pareto front with different hot inlet temperatures

Figure 7 provides a detailed analysis of Thermoelectric Generator (TEG) configurations, focusing on the trade-offs between maximum output power, total power, and conversion efficiency. In Figure 7(a), series configurations connect TEGs end-to-end, enhancing voltage and efficiency but introducing higher resistance, which limits power output. Parallel configurations, connecting TEGs side-by-side, reduce resistance and increase power output, though they may be less efficient due to suboptimal use of the thermal gradient. Figure 7(b) explores the impact of channel width. In parallel setups, narrower channels with fewer TEGs improve power and efficiency by optimizing heat transfer and reducing resistance. Wider channels with more TEGs decrease performance due to increased resistance. For series configurations, wider channels enhance power by distributing heat better but

reduce efficiency due to cumulative resistance. Narrower channels improve efficiency but limit heat absorption, reducing power output. Figure 7(c) discusses channel length. Shorter channels reduce pressure drop and improve efficiency but lower power output. Longer channels increase power output but also raise pressure drop, which can reduce efficiency. Overall, balancing TEG configuration, channel width, and length is crucial for optimizing both power and efficiency.

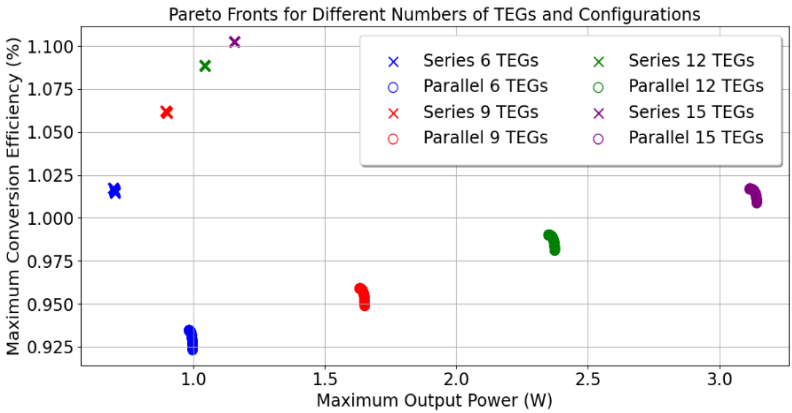

(a)

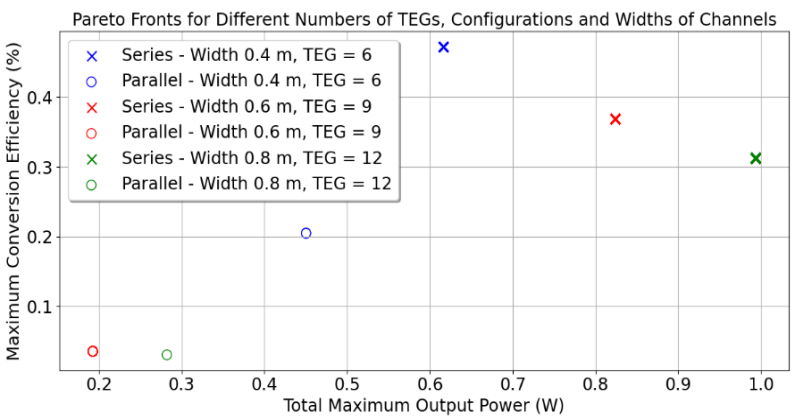

(b)

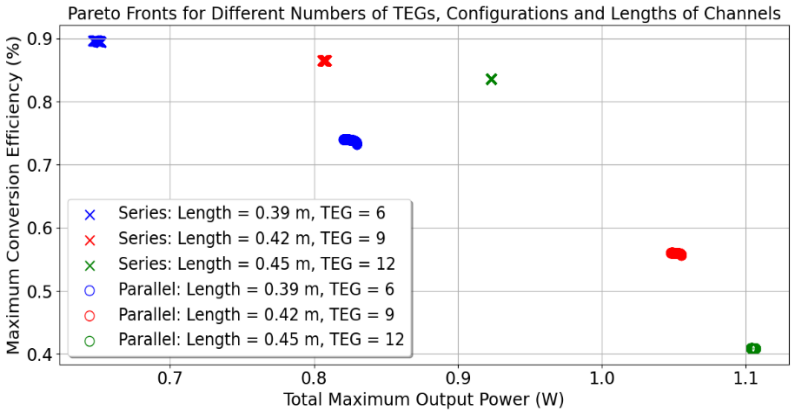

(c)

Figure 7: Pareto front analysis using a different (a) number of TEGs and configurations alongside different (b) width and (c) length of channels

Conclusions

This study utilized the NSGA-II algorithm to optimize PFHEs in TEGs, achieving a 3.94% increase in maximum output power (from 0.137 W to 0.1424 W) and a 1.72% increase in efficiency (from 0.95% to 0.9663%). The optimized design, featuring 64 fins, also increased the total maximum output power for three TEGs from 0.411 W to 0.4272 W, a 3.94% improvement. At the highest tested temperature of 428.15 K, the system reached a maximum conversion efficiency of 2.42% and a maximum output power of 0.89 W, representing increases of 154.74% and 549.64%, respectively. Convergence analysis and hypervolume indicators validated the robustness of the NSGA-II algorithm. These findings underscore the need to balance design parameters for optimal performance and demonstrate the effectiveness of AI-driven optimization in enhancing waste heat recovery. The optimization process was completed in just 14 minutes, efficiently handling 7,500 iterations, and significantly reducing computational time and resources.

Contributions of Authors

The authors confirm the equal contribution in each part of this work. All authors reviewed and approved the final version of this work.

Funding

This work received funding for publication from the Office of Management and Human Resources, College of Engineering, Universiti Teknologi MARA, Shah Alam, Malaysia.

Conflict of Interests

One of the authors, Baljit Singh Bhathal Singh is a section editor of the Journal of Mechanical Engineering (JMechE). The author has no other conflict of interest to note.

Acknowledgment

This research was funded by Universiti Teknologi MARA Geran Kolaborasi Entiti Penyelidikan UiTM (KEPU) numbered 600-RMC/KEPU 5/3 (014/2021). The authors would also like to express their gratitude to the Office of Management and Human Resources, College of Engineering, Universiti Teknologi MARA, Shah Alam, Malaysia, for their financial support towards the publication of this work.

References

[1] J. S. Khan, I. Ahmad, U. K. Jadoon, A. Samad, H. Saghir, M. Kano, and H. Caliskan, "Artificial intelligence based prediction of optimum operating conditions of a plate and fin heat exchanger under uncertainty: A gray-box approach," *International Journal of Heat and Mass Transfer*, vol. 217, no. 6, p. 124653, 2023. https://doi.org/10.1016/j.ijheatmasstransfer.2023.124653

[2] Z. Miao, X. Meng, and X. Li, "Design a high-performance thermoelectric generator by analyzing industrial heat transfer," *Applied Energy*, vol. 347, p. 121403, 2023. https://doi.org/10.1016/j.apenergy.2023.121403

[3] N. Nourdanesh and A. Kantzas, "Using Thermoelectric Generators (TEGs) for Electric Power Generation from Waste Heat in Geothermal Plants," *SPE Canadian Energy Technology Conference and Exhibition*, pp. 1–2, 2023. https://doi.org/10.2118/212748-ms

[4] K. S. Garud, J. Seo, M. S. Patil, Y. Bang, Y. Pyo, C. Cho, and M. Lee, "Thermal–electrical–structural performances of hot heat exchanger with different internal fins of thermoelectric generator for low power generation application," *Journal of Thermal Analysis and Calorimetry*,

vol. 143, no. 1, p. 388, 2020. https://doi.org/10.1007/s10973-020-09553-7

[5] William L. Hosch, "*Genetic Algorithm*," Aug 5, 2024. [Online]. Available: https://www.britannica.com/technology/genetic-algorithm (Accessed: Dec 13, 2023).

[6] S. Katoch, S. S. Chauhan, and V. Kumar, "A review on genetic algorithm: past, present, and future," *Multimedia Tools and Applications*, vol. 80, no. 5, pp. 8091–8092, 2021. https://doi.org/10.1007/s11042-020-10139-6

[7] R. Song and M. Cui, "Single- and multi-objective optimization of a plate-fin heat exchanger with offset strip fins adopting the genetic algorithm," *Applied Thermal Engineering*, vol. 159, pp. 1–2, 2019. https://doi.org/10.1016/j.applthermaleng.2019.113881

[8] L. Meng, J. Liu, J. Bi, E. D. Özdemir, and M. H. Aksel, "Multi-objective optimization of plate heat exchanger for commercial electric vehicle based on genetic algorithm," *Case Studies in Thermal Engineering*, vol. 41, no. 8, p. 102629, 2023. https://doi.org/10.1016/j.csite.2022.102629

[9] M. Darvish Damavandi, M. Forouzanmehr, and H. Safikhani, "Modeling and Pareto based multi-objective optimization of wavy fin-and-elliptical tube heat exchangers using CFD and NSGA-II algorithm," *Applied Thermal Engineering*, vol. 111, pp. 325–327, 2017. https://doi.org/10.1016/j.applthermaleng.2016.09.120

[10] H. Hajabdollahi, P. Ahmadi, and I. Dincer, "Exergetic Optimization of Shell-and-Tube Heat Exchangers Using NSGA-II," *Heat Transfer Engineering*, vol. 33, no. 7, pp. 621–626, 2012. https://doi.org/10.1080/01457632.2012.630266

[11] Y. Wang, J. Li, W. Liu, J. Dong, and J. Liu, "Integrating NSGA-II and CFD for enhanced urban airflow prediction: Recalibration of closure coefficients for a nonlinear eddy viscosity model," *Building and Environment*, vol. 259, pp. 1–16, 2024. https://doi.org/10.1016/j.buildenv.2024.111627

[12] F. Zhu, Y. Liu, C. Lu, Q. Huang, and C. Wang, "Research on thermal energy management for PHEV based on NSGA-II optimization algorithm," *Case Studies in Thermal Engineering*, vol. 54, pp. 1–13, 2024. https://doi.org/10.1016/j.csite.2024.104046

[13] S. Lan, Z. Yang, R. Stobart, and R. Chen, "Prediction of the fuel economy potential for a skutterudite thermoelectric generator in light-duty vehicle applications," *Applied Energy*, vol. 231, pp. 68–71, 2018. https://doi.org/10.1016/j.apenergy.2018.09.087

[14] Y. Zhu, D. W. Newbrook, P. Dai, C. H. K. de Groot, and R. Huang, "Artificial neural network enabled accurate geometrical design and optimisation of thermoelectric generator," *Applied Energy*, vol. 305, p. 2, 2022. https://doi.org/10.1016/j.apenergy.2021.117800

[15] W. H. Chen, Y. Bin Chiou, R. Y. Chein, J. Y. Uan, and X. D. Wang, "Power generation of thermoelectric generator with plate fins for recovering low-temperature waste heat," *Applied Energy*, vol. 306, no. 2, pp. 1–19, 2022. https://doi.org/10.1016/j.apenergy.2021.118012

[16] S. Zou, E. Kanimba, T. E. Diller, Z. Tian, and Z. He, "Modeling assisted evaluation of direct electricity generation from waste heat of wastewater via a thermoelectric generator," *The Science of the Total Environment*, vol. 635, pp. 1215–1217, 2018. https://doi.org/10.1016/j.scitotenv.2018.04.201

[17] W. He, S. Wang, C. Lu, Y. Li, and X. Zhang, "An Optimization Analysis of Thermoelectric Generator Structure for Different Flow Directions of Working Fluids," *Energy Procedia*, vol. 61, pp. 718–721, 2014. https://doi.org/10.1016/j.egypro.2014.11.950

[18] M. Chen, L. A. Rosendahl, and T. Condra, "A three-dimensional numerical model of thermoelectric generators in fluid power systems," *International Journal of Heat and Mass Transfer*, vol. 54, no. 1–3, pp. 345–355, 2011. https://doi.org/10.1016/j.ijheatmasstransfer.2010.08.024

[19] J.-Y. Jang, Y.-C. Tsai, and C.-W. Wu, "A study of 3-D numerical simulation and comparison with experimental results on turbulent flow of venting flue gas using thermoelectric generator modules and plate fin heat sink," *Energy*, vol. 53, pp. 270–281, 2013. https://doi.org/10.1016/j.energy.2013.03.010

[20] M. V. V. Mortean and M. B. H. Mantelli, "Nusselt number correlation for compact heat exchangers in transition regimes," *Applied Thermal Engineering*, vol. 151, p. 515, 2019. https://doi.org/10.1016/j.applthermaleng.2019.02.017

[21] J. Blank and K. Deb, "Pymoo: Multi-Objective Optimization in Python," *IEEE Access*, vol. 8, pp. 89497–89509, 2020. https://doi.org/10.1109/access.2020.2990567

[22] K. Deb, A. Pratap, S. Agarwal, and T. Meyarivan, "A fast and elitist multiobjective genetic algorithm: NSGA-II," *IEEE Transactions on Evolutionary Computation*, vol. 6, no. 2, pp. 183–186, 2002. https://doi.org/10.1109/4235.996017

[23] C. Wang, Z. Cui, H. Yu, K. Chen, and J. Wang, "Intelligent optimization design of shell and helically coiled tube heat exchanger based on genetic algorithm," *International Journal of Heat and Mass Transfer*, vol. 159, no. 9-10, pp. 4–5, 2020. https://doi.org/10.1016/j.ijheatmasstransfer.2020.120140

[24] G. F. Peixer, A. T. D. Nakashima, J. A. Lozano, and J. R. Barbosa, "System-level multi-objective optimization of a magnetic air conditioner through coupling of artificial neural networks and genetic algorithms," *Applied Thermal Engineering*, vol. 227, pp. 14–15, 2023. https://doi.org/10.1016/j.applthermaleng.2023.120368

[25] R. T. Marler and J. S. Arora, “Survey of multi-objective optimization methods for engineering,” *Structural and Multidisciplinary Optimization*, vol. 26, no. 6, pp. 371–389, 2004. https://doi.org/10.1007/s00158-003-0368-6